

## Frequency dependent radio structure of the gravitational lens system B0218+357

Alok R. Patnaik and Richard W. Porcas

*Max-Planck-Institut für Radioastronomie, Auf dem Hügel 69, D 53121 Bonn, Germany.*

**Abstract.** We present multi-frequency radio continuum VLBI observations of the gravitational lens system B0218+357 carried out using a global VLBI network and the VLBA. The source has been observed with resolutions from 0.2 mas to 5 mas and displays interesting structure. The spectral properties of various components show that the lensed object is a standard flat spectrum radio source which has many self-absorbed components. Based on the flux ratio of the lensed images as a function of frequency we propose a simple model for the background radio source.

### 1. Introduction

The radio source B0218+357 has been identified as a gravitationally lensed system (Patnaik et al. 1993). The source, which has a core-halo structure at low frequency (1.4 GHz) and low resolution (5 arcsec), consists of two compact flat-spectrum components, A and B, separated by 335 milliarcsec. The weaker of the two, B, is surrounded by a faint Einstein ring of similar diameter. The spectral and polarisation characteristics of the components show them to be the lensed images of a single flat spectrum ‘core’. The lensing galaxy, suggested to be a spiral galaxy, has been observed by the HST (Jackson et al. 1997). It has a redshift of 0.6847 (Browne et al. 1993). Atomic hydrogen and many molecular species have been detected in absorption against the background source (Carilli et al. 1993, Wiklind & Combes 1995, Menten & Reid 1996). The redshift of the background object is suggested to be 0.96 (Lawrence 1996).

In this contribution we explore the properties of the radio source from our multi-frequency VLBI observations. We give a summary of our observations and discuss the results in the context of a flat spectrum radio source. We note that the overall radio spectrum of B0218+357 is flat between 365 MHz and 43 GHz i.e. its flux density is constant within a factor of two between these frequencies.

### 2. Observations

B0218+357 has been observed at 1.7, 5, 15, 22 and 43 GHz over the last several years in order to understand its small-scale structure and thereby derive constraints for the lens models. The 1.7 and 5 GHz observations were carried out in 1992 with a global array using the MK3 VLBI system and the VLBA was used for the higher frequency observations. About 10 telescopes were used

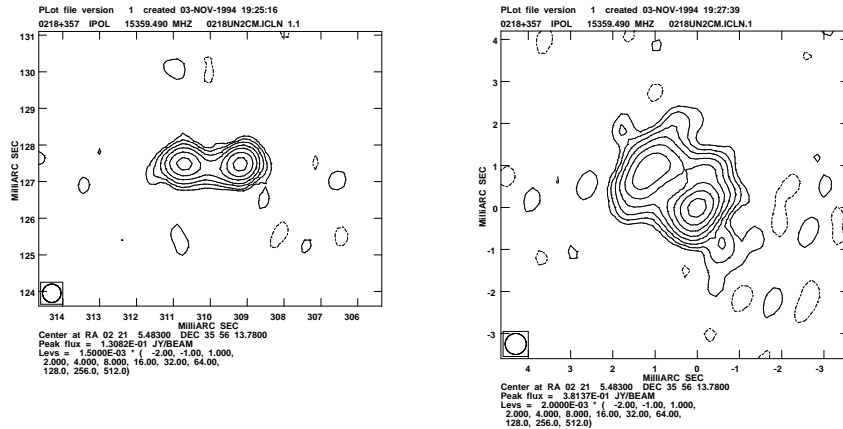


Figure 1. 15 GHz VLBA maps of B0218+357 images A (right) and B (left) with a resolution of 0.5 mas. The contour levels for image B are  $1.5 \text{ mJy/beam} \times (-1, 1, 2, 4, 8, 16, 32, 64, 128)$  and the peak flux density is  $130.8 \text{ mJy/beam}$ . The contour levels for image A are  $2.0 \text{ mJy/beam} \times (-1, 1, 2, 4, 16, 32, 64, 128, 256)$  and the peak flux density is  $381.4 \text{ mJy/beam}$ . The restoring beam of size 0.5 mas is drawn in the bottom left hand corner of each panel. The tick interval is 1 mas. Component 1 is the western component in each image.

in each of the observing sessions. The global array data were correlated at the MPIfR, Bonn. The data at 15, 22 and 43 GHz were taken using the VLBA with a bandwidth of 64 MHz. The data were kept in 8 MHz channels to avoid bandwidth smearing. The data were analysed using the NRAO AIPS software package.

### 3. Results

The 1.7, 5 and 15 GHz maps are published by Porcas & Patnaik (1996a), another 15 GHz map and 22 and 43 GHz maps are published by Porcas & Patnaik (1996b). In this contribution we show a 15 GHz map (Patnaik, Porcas & Browne 1995) to identify the different components (Fig. 1).

At resolutions around a few milliarcsec we are not sensitive to extended emission from the Einstein ring. At resolutions higher than about 1 mas, which is achieved for frequencies higher than 8.4 GHz, each of the lensed images, A and B, is resolved into a ‘core-jet’ structure (Fig. 1). We identify A1 (the southwestern component of A) and its lensed counterpart B1 (the western component of B) as the core of the background radio source. Correspondingly, A2 and B2 are identified as part of the jet. This identification is justified from the fact that A1 and B1 have flatter spectra than A2 and B2 (Table 1, Fig. 2) and also from the fact that they are unresolved at 43 GHz with a resolution of 0.2 mas.

The images A and B have diffuse structure at 1.7 and 5 GHz such that it is difficult to match corresponding features in them. Image A shows characteristic ‘tangential’ elongation in PA  $-40^\circ$ . This elongation is also seen at higher fre-

quencies. The other noticeable feature is the rather dramatic increase in size of image A and B with wavelength. Even though the sizes of the images increase with decreasing frequency, their surface brightnesses at low levels are the same as expected from gravitational lensing.

Table 1. Flux densities (in mJy) of components in B0218+357.

Frequency	Date	Resolution in mas	A	B	A1	B1	A2	B2
1.7GHz	1992 Jun 19	5	445	170	-	-	-	-
5.0GHz	1992 Mar 27	1	515	196	-	-	-	-
8.4GHz	1995 May 09	1	-	-	472	139	218	63
15 GHz	1995 Jul 17	0.5	-	-	450	295	121	66
22GHz	1995 Jul 17	0.3	-	-	328	140	100	41
43GHz	1995 Jul 17	0.2	-	-	270	60	75	22

Table 1 summarises the results of the multi-frequency VLBI observations. The flux densities of various components (identified in Fig.1) are plotted in Fig.2.

#### 4. Discussion

We derive two basic results from these observations, namely the spectral decomposition of various components and the ratio of their flux densities as a function of frequency.

Since we resolve the ‘core-jet’ structure in A and B at frequencies higher than 8.4 GHz, we have 4 measurements of flux density for these components. The spectra are plotted in Fig. 2. The spectrum of the core (A1 and B1) is self-absorbed with a peak around 15 GHz. The jet (A2 and B2) has steep spectra above 8.4 GHz. However, the total flux density of A and B at 1.7 and 5 GHz suggest that both A2 and B2 must also be self-absorbed between these two frequencies. The Einstein ring emission has a steeper spectrum between 5 and 22 GHz and it must also be self-absorbed at lower frequencies since the total flux density provides a limit (Patnaik et al. 1993).

In summary, the radio structure of B0218+357 consists of at least 3 distinct components, core, jet and the Einstein ring, which are all self-absorbed at different frequencies. The components are self-absorbed at progressively lower frequencies as one moves from the core along the jet. This behaviour of the radio source is consistent with its flat spectrum (Cotton et al. 1980).

The core, being self-absorbed around 15 GHz, contributes very little to the emission at 1.7 and 5 GHz, where the emission is dominated by the jet as evident from the spectra. Perhaps it is not surprising therefore that the radio structures of both A and B at 1.7 GHz appear diffuse. However, this poses a difficulty in that a self-absorbed component, which must be compact, has a large observed size. In this case one must consider the intrinsic size of the source rather than the observed size which has been magnified by the lens.

Another result from our observations is that the image flux ratios change with frequency. This is an apparent contradiction since gravitational lensing is achromatic. However, since the source is extended and spans areas of different

Spectrum of B0218+357

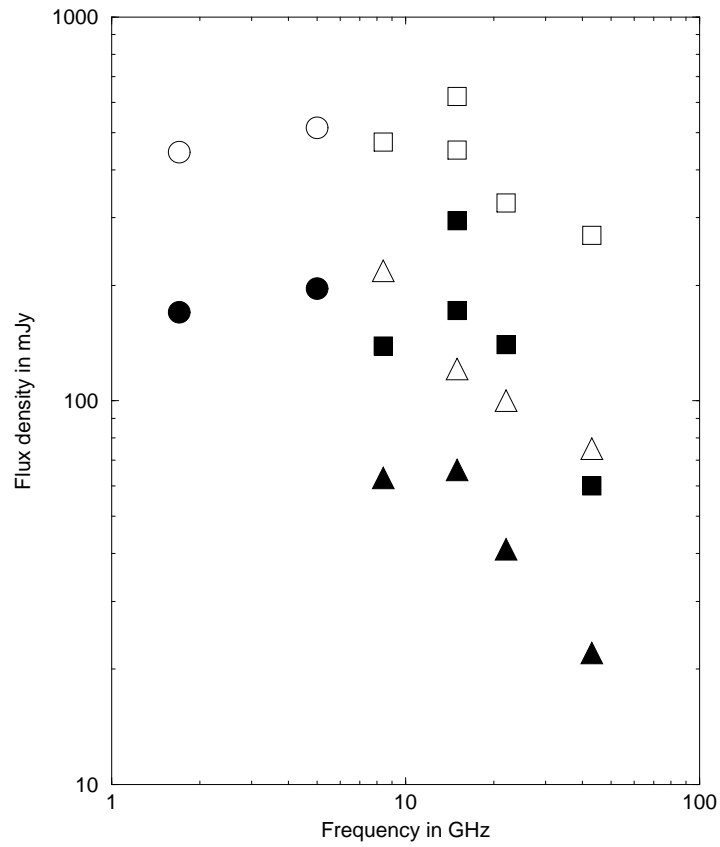


Figure 2. Spectrum of B0218+357. The various symbols are: open circle: A; open square: A1; open triangle: A2; filled circle: B; filled square: B1; filled triangle: B2. The errors on the flux densities are expected to be about 5%. However, the flux ratios are more accurate.

image magnifications the observed flux ratio can indeed vary with frequency. The flux ratio of the core (i.e. A1/B1) is around 3.7 for frequencies higher than 8.4 GHz. This is similar to the ratio of A/B obtained from VLA observations at these frequencies (Patnaik et al. 1993). At lower frequencies the flux ratio A/B is around 2.6. Of course, we point out that the source is variable at high frequencies and thus the measured flux ratio can be different due to differential time delay.

The above results lead to a rather simple model for B0218+357. The radio source consists of a number of different components which are self-absorbed at different frequencies thus conspiring to produce the observed flat spectrum. The core (imaged into A1 and B1) is located at the western-most edge, the jet (imaged into A2 and B2) lies between the core and the component giving rise to the Einstein ring. The core dominates the radio structure at frequencies higher than 8.4 GHz, and the jet and the Einstein ring dominate at lower frequencies. At lower frequencies one does not detect any compact feature in the source since the core contributes very little to the flux density.

**Acknowledgments.** We would like to thank Athol Kemball for allowing us to quote results before publication and Karl Menten for his comments. The Very Long Baseline Array of NRAO is operated by AUI under cooperative agreement with the NSF, USA.

## References

- Browne, I.W.A., Patnaik, A.R., Walsh, D. & Wilkinson, P.N., 1993, MNRAS, 263, L32
- Carilli, C.L., Rupen, M.P. & Yanny, B., 1993, ApJ, 412, L59
- Cotton, W.D., Wittels, J.J., Shapiro, I.I., Marcaide, J., Owen, F.N., Spangler, S.R., Rius, A., Angulo, C., Clark, T.A. & Knight, C.A., 1980, ApJ, 238, 123
- Jackson, N., Nair, S. & Browne, I. 1997, in Cosmology with the new radio surveys, eds Bremer, M. & Jackson, N.J., p315
- Lawrence, C.R., 1996, in IAU Symp. 173, eds Kochanek, C.S. & Hewitt, J.N., Dordrecht: Kluwer, 299
- Menten, K.M. & Reid, M.J., 1996, ApJ, 465, L99
- Patnaik, A.R., Browne, I.W.A., King, L.J., Muxlow, T.W.B., Walsh, D. & Wilkinson, P.N., 1993, MNRAS, 261, 435
- Patnaik, A.R., Porcas, R.W. & Browne, I.W.A, 1995, MNRAS, 274, L5
- Porcas, R.W. & Patnaik, A.R., 1996a, in IAU Symp. 173, eds Kochanek, C.S. & Hewitt, J.N., Dordrecht: Kluwer, 311
- Porcas, R.W. & Patnaik, A.R., 1996b, in IAU Symp. 175, eds Ekers, R., Fanti, C. & Padrielli, L., Dordrecht: Kluwer, 115
- Wiklind, T. & Combes, F., 1995, A&A, 299, 382